International Journal of Mechanical System Dynamics

WILEY

IJMSD International Journal of Mechanical System Dynamics Open Access

RESEARCH ARTICLE OPEN ACCESS

A Multi-Mode Analytical Frequency Modulation Input-Shaping Control

Khaled Alhazza

Department of Mechanical Engineering, Kuwait University, Alshedadia, Kuwait

Correspondence: Khaled Alhazza (Khaled.alhazza@ku.edu.kw; kalhazza@vt.edu)

Received: 15 January 2025 | **Revised:** 13 February 2025 | **Accepted:** 24 February 2025

Funding: The study was supported by the Kuwait University Research Sector (EM04/24).

Keywords: crane control | frequency modulation | modified double step | multimode shaper

ABSTRACT

In rest-to-rest maneuvers, input shapers like the double step (DS), zero vibration (ZV), and zero vibration derivative (ZVD) are widely utilized to eliminate residual vibrations in single-mode systems. These shapers can be used to eliminate residual oscillations in multimode systems, given that the higher frequencies are odd multiples of the system's fundamental frequency. However, the natural frequencies depend on the physical properties of the system, and such ratios cannot be guaranteed. In this study, an analytical frequency modulation technique is proposed to eliminate the residual oscillations of a double pendulum using a modified single-mode shaper. The proposed technique is based on altering the natural frequencies of the system, forcing the odd multiple ratio. This involves modifying a single-mode double-step (SMDS) input shaper by adding scaled state variables, first and second angles, to the original shaper. This addition allows the user to choose the first natural frequency and force the second natural frequency to be an odd multiple of the chosen frequency. To apply the proposed technique, the double pendulum nonlinear equations of motion are derived, linearized, and then solved analytically using modal analysis. The scaling parameters used to modify the natural frequencies are then solved analytically. To prove the concept, several numerical simulations with randomly selected parameters are presented and then experimentally tested on a scaled overhead crane. The numerical and experimental results demonstrate the effectiveness of the proposed technique.

1 | Introduction

Rest-to-rest maneuvers are widely used in industrial operations. Many control techniques are suggested to enhance safety, reduce maintenance, and/or reduce maneuvering time [1–3]. These control techniques are mainly feedback, open loop, or a combination of the two techniques. Feedback techniques are usually more robust; however, implementing such controller techniques may require altering the existing system by adding sensors and/or actuators. However, open-loop control techniques, which do not require system alteration, cannot tolerate disturbances during operation. To go beyond the limitations of the two control approaches, researchers tend to integrate feedback and command-shaping techniques [4, 5].

Due to their effectiveness, input- and command-shaping techniques, both categorized as open-loop control techniques, are two of the most recommended and utilized maneuvers in modern industry. Open-loop techniques are based on predefining the motion trajectory to eliminate residual vibrations at the end of maneuvers. In recent decades, many input and command-shaping techniques have been developed, studied, and analyzed [1–3]. These studies were expanded to numerous applications, including microbeams, dielectric actuators, and hard-magnetic actuators [6–9].

Early shapers started by dividing a constant ON/OFF command into two stages, separated by half the payload's oscillation duration [1, 2]. This generates the double step (DS) and

zero-vibration (ZV) input shapers. Trying to understand and modify these controllers, Singhose et al. [10, 11] focused on the smoothness of the input command profiles, the robustness, the maneuver speed, transient oscillations, and the ease of implementation. Considering the effect of first-order actuators, Sung and Lee [12] analytically proposed a zero-vibration-derivative (ZVD) shaper using a phasor-vector approach.

Using variable acceleration profiles, several waveform command shapers for rest-to-rest maneuvers were suggested and implemented [13, 14]. Waveform command shapers are utilized numerically and experimentally to effectively eliminate residual vibrations in both single-mode and multi-mode systems. Furthermore, waveform command shapers are among the fastest shaping techniques, sometimes surpassing the ZV input shaper [15]. Extending the work on command shaping, the effects of damping and hoisting were considered [16, 17]. The nonzero initial conditions and system inclination were also studied [18–22].

When dealing with large payloads or relatively heavy hooks, the assumption of a single mode is inaccurate, as it fails to eliminate all induced vibrations, particularly in the higher modes. For such cases, the system must be treated as a double pendulum to eliminate all unwanted vibrations. The dynamics and stability of double pendulums have been extensively studied by many researchers [23–27]. Most research on input- and command-shaping techniques has focused on single-mode systems [1–3]. However, single-mode shapers can not eliminate the vibrations induced in multi-mode systems or large payloads. Disregarding such a fact may result in substantial unwanted vibrations.

To overcome this deficiency, various strategies have been employed to reduce vibrations in higher modes, including notch and low-pass filters, delays, band-stop filters, and multi-mode command shapers [28–34]. To facilitate the application of single-mode shapers in multi-mode systems, researchers [35–37] used numerical model-based feedback to adjust higher mode frequencies to odd multiples of the fundamental mode frequency. They employed a complex feedback mechanism with unspecified variables in their research. Using similar approaches, Arabasi and Masoud [38, 39] implemented numerical model-based feedback input-shaper combined with frequency modulation to control the residual vibrations of simultaneous hoist and travel maneuvers in double pendulum overhead cranes. Alhazza [40] effectively controls oscillations in multi-mode systems using a modified single-mode command-shaping utilizing the lower angle of the double pendulum. The effectiveness of the proposed shaper has been shown through two numerical simulations.

An analytically derived single-mode double-step input shaper is modified and then utilized to reduce residual vibrations using a frequency modulation approach. It is well known that single-mode double-step (SMDS) input shapers can effectively eliminate residual vibrations in a multi-mode system, provided that all higher frequencies are odd multiples of the fundamental frequency of the shaped command. Based on this fact, an analytically driven new command-shaping technique is developed to eliminate residual vibrations in multimode systems. Our approach involves convolving the original SMDS command with scaled first- and second-state variables. The added scaled state variables give the ability to set the fundamental frequency and force the upper frequency to be an odd multiple of the fundamental frequency. This modification of the system's frequencies slightly alters the shaper's acceleration, velocity, and displacement profiles to significantly reduce the residual vibrations. To validate the proposed technique, four numerically simulated and experimentally performed examples with arbitrarily chosen parameters are shown and discussed. Through experiments and simulations, the results clearly show that the proposed shaper can effectively eliminate first- and second-mode vibrations in the double pendulum system. It is worth noting that the proposed shaper can be implemented on other multi-mode systems with linear ordinary differential equations.

2 | Mathematical Model

In most cases, an overhead crane can be represented as a two-degree-of-freedom system with two-point masses linked to the crane trolley. These masses physically signify the hook and payload. In Figure 1, the initial mass of the double pendulum is attached to a horizontally traversing trolley or jib by a fixed length cable l_1. This mass is connected to a second mass by a fixed-length cable l_2. The nonlinear equations of motion for the simplified system can be theoretically articulated as [23, 25]

$$\begin{aligned}(m_1+m_2)\left[l_1^2\ddot{\theta}+l_1 g\sin(\theta)\right]+m_2 l_1 l_2[\ddot{\phi}\cos(\theta-\phi)\\ +\dot{\phi}^2\sin(\theta-\phi)]=(m_1+m_2)l_1\cos(\theta)\ddot{u}\end{aligned}, \tag{1}$$

$$\begin{aligned}m_2 l_2^2\ddot{\phi}+m_2 l_2\ddot{l}_1\sin(\theta-\phi)-m_2 l_2 l_1[\dot{\theta}^2\sin(\theta-\phi)\\ -\ddot{\theta}\cos(\theta-\phi)]+2m_2 l_2\dot{l}_1\dot{\theta}\cos(\theta-\phi)\\ +m_2 g l_2\sin(\phi)=m_2 l_2\cos(\phi)\ddot{u}\end{aligned}. \tag{2}$$

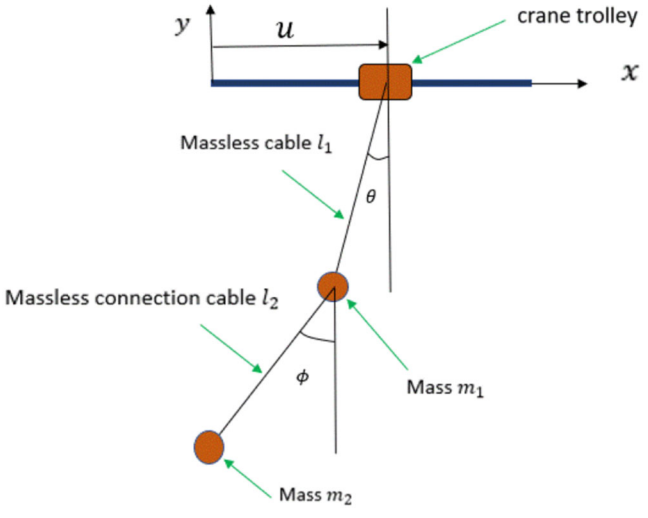

FIGURE 1 | A simplified double pendulum, with two point masses, attached to an overhead crane trolley.

It is well known that for nonlinear equations, an exact analytical solution cannot be derived analytically. Most of the work done on input and command shaping technique linearized the equations of motion under the small angle approximation (i.e., θ and $\phi \ll 1$) [1–3]. The validity of this approximation is proven both numerically and experimentally in many studies. To find an analytical solution, the equations of motion are linearized and solved analytically for the shaper constants to achieve zero residual vibrations. Examining Equations (1) and (2), the linearized equations of motion may be expressed in matrix form as

$$\boldsymbol{M}\ddot{\boldsymbol{\Phi}} + \boldsymbol{K}\boldsymbol{\Phi} = \boldsymbol{B}\ddot{u}, \tag{3}$$

where

$$\boldsymbol{M} = \begin{bmatrix} l_1^2(m_1 + m_2) & m_2 l_1 l_2 \\ m_2 l_1 l_2 & m_2 l_2^2 \end{bmatrix} \tag{4}$$

$$\boldsymbol{K} = \begin{bmatrix} l_1 g(m_1 + m_2) & 0 \\ 0 & g m_2 l_2 \end{bmatrix} \tag{5}$$

$$\boldsymbol{B} = \begin{bmatrix} l_1(m_1 + m_2) \\ l_2 m_2 \end{bmatrix} \tag{6}$$

$$\boldsymbol{\Phi} = \begin{bmatrix} \theta \\ \phi \end{bmatrix}. \tag{7}$$

3 | Shaper Design

It is worth mentioning that the shaper design in this section is devoted to the acceleration phase of the shaper. It is important to explain the basic concept of the rest-to-rest maneuver to better understand the proposed technique. In this maneuver, the trolley goes through three main phases: acceleration, cruise, and deceleration. In the acceleration phase, the trolley starts from rest and accelerates to reach maximum velocity. To reduce or eliminate residual vibrations, input shaping or command shaping is designed in the acceleration phase, ensuring zero vibrations at the end of this phase. In the second stage, the trolley moves with a constant cruising velocity. Due to the absence of acceleration in this phase, the velocity remains invariant, that is, no new induced vibration is introduced. To end the maneuver, the trolley is decelerated to stop at the end of the deceleration phase using an inverted acceleration profile; see Figure 2.

In this study, a modified classical SMDS shaper is used to suppress oscillations in all modes of the multimode system. It is worth noting that various classical single-mode input shapers, such as ZV or ZVD, may be used as principal command shapers in this approach. To better understand the single-mode double-step input shaper used in this study, the acceleration phase in the time-optimal rigid-body (TORB) profile is split into two stages. The timing of these steps is synchronized, and the second step is specifically designed to counteract the impact caused by the first step. A comparison between the two shapers with stage timing is shown in Figure 2.

The acceleration of the (SMDS) shaper can be expressed mathematically as

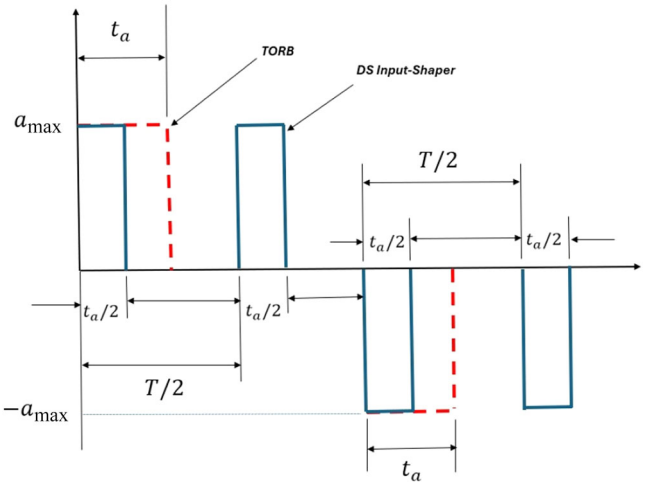

FIGURE 2 | Time optimal rigid body (TORB) and single-mode double-step (SMDS) command shaper acceleration profiles.

$$\ddot{u} = \begin{cases} a_{\max} & 0 < t < t_a/2 \\ 0 & t_a/2 < t < T/2 \\ a_{\max} & T/2 < t < T/2 + t_a \end{cases}, \tag{8}$$

where T represents the period of the fundamental frequency and t_a denotes the total acceleration time of the (TORB) command. This form of input shaping has been proven numerically and experimentally to eliminate residual vibrations in single-mode systems. Moreover, it can suppress residual vibrations in all modes, given that higher modes are odd multiples of the system's fundamental frequency. To take advantage of this advantage, the system's first and second state variables, θ and ϕ, are merged with the double-step acceleration profile to modulate the system frequencies. The modified acceleration can be mathematically written as

$$\hat{u}\ = \begin{cases} a_{\max} + C\theta + D\phi & 0 < t < t_a \\ C\theta + D\phi & t_a/2 < t < T/2 \\ a_{\max} + C\theta + D\phi & T/2 < t < T/2 + t_a \end{cases}, \tag{9}$$

Substituting the proposed modified acceleration (9) into the linear equation of motion (3), and rearranging the equations in matrix form gives

$$\boldsymbol{M}\ddot{\boldsymbol{\Phi}} + \hat{\boldsymbol{K}}\,\boldsymbol{\Phi} = \boldsymbol{B}\ddot{u} \tag{10}$$

where

$$\boldsymbol{M} = \begin{bmatrix} l_1^2(m_1 + m_2) & m_2 l_1 l_2 \\ m_2 l_1 l_2 & m_2 l_2^2 \end{bmatrix} \tag{11}$$

$$\hat{\boldsymbol{K}} = \begin{bmatrix} l_1(g - C)(m_1 + m_2) & -l_1 D(m_1 + m_2) \\ -m_2 l_2 C & m_2 l_2 (g - D) \end{bmatrix} \tag{12}$$

$$\boldsymbol{B} = \begin{bmatrix} l_1(m_1 + m_2) \\ l_2 m_2 \end{bmatrix}. \tag{13}$$

where $\hat{\boldsymbol{K}}$ is the modified stiffness matrix. It is clear that the scaled constants only affected the stiffness matrix $\hat{\boldsymbol{K}}$, which alters the system's frequencies with no effect on damping. To solve the system using modal analysis, the eigenvalues or natural frequencies of the system, (10), can be found as

$$\omega_{1,2}^2 = \frac{g(l_1+l_2)m_t}{2l_1l_2m_1} - \frac{C}{2l_1} \mp \frac{1}{2l_1l_2m_1}\sqrt{g^2[(l_1+l_2)^2m_t^2 - 4l_1l_2m_1m_t] + f(C) + f(D)} \tag{14}$$

where

$$f(C) = C^2l_2^2m_1^2 + 2gCl_2m_1(l_1-l_2)(m_1+m_2) \tag{15}$$

$$f(D) = 4l_1l_2m_1g(m_1+m_2)D \tag{16}$$

and

$$m_t = (m_1+m_2). \tag{17}$$

It is clear from Equation (14) that the scaling factors C and D can be utilized to control the first and second natural frequencies, $\omega_{1,2}$. Since two equations can be used to alter both frequencies, two constraints are required. It is worth noting that the constraints can be changed depending on the purpose of the research. The proposed shaper gives the freedom to choose both frequencies independently. In this study, the first constraint chooses the first natural frequency, while the second constraint is to make the second natural frequency an odd multiple of the fundamental frequency. These constraints are expressed mathematically as

$$\omega_1 = \bar{\omega}_1 \tag{18}$$

$$n = \frac{\omega_2}{\bar{\omega}_1} \quad n = 3, 5, 7, \ldots \tag{19}$$

It is worth noting that n can have any value; however setting n as an odd number utilizes the advantage of the double-step input shaper to eliminate all induced vibrations in multimode systems. Substituting Equation (14) into the constraints Equations (18) and (19), with simple mathematical manipulations, the values of C and D are expressed analytically as

$$C = -l_1(n^2+1)\bar{\omega}_1^2 + \frac{(l_1+l_2)(m_1+m_2)g}{l_2m_1} \tag{20}$$

$$D = -\frac{n^2l_1l_2m_1\bar{\omega}_1^4}{g(m_1+m_2)} + l_1(n^2+1)\bar{\omega}_1^2 - \frac{[l_1(m_1+m_2)+l_2m_2]g}{l_2m_1}. \tag{21}$$

To find an analytical solution of the state variables, θ and ϕ, the mode shapes are written as

$$\boldsymbol{\theta} = \begin{bmatrix} 1 \\ \psi_1 \end{bmatrix} \tag{22}$$

$$\boldsymbol{\Phi} = \begin{bmatrix} 1 \\ \psi_2 \end{bmatrix} \tag{23}$$

where

$$\psi_1 = -\frac{(m_1+m_2)(\omega_1^2l_1 + C - g)}{(m_1+m_2)D + \omega_1^2l_2m_2} \tag{24}$$

$$\psi_2 = -\frac{(m_1+m_2)(\omega_2^2l_1 + C - g)}{(m_1+m_2)D + \omega_2^2l_2m_2}. \tag{25}$$

Using Equations (22)–(25), the general solution of the two-degree-of-freedom system can be written as

$$\theta(t) = U_{11}\sin(\omega_1 t) + U_{12}\cos(\omega_1 t) + U_{21}\sin(n\omega_1 t) + U_{22}\cos(n\omega_1 t) - \frac{a_{\max}}{C+D-g} \tag{26}$$

$$\phi(t) = \psi_1(U_{11}\sin(\omega_1 t) + U_{12}\cos(\omega_1 t)) + \psi_2(U_{21}\sin(n\omega_1 t) + U_{22}\cos(n\omega_1 t)) - \frac{a_{\max}}{C+D-g} \tag{27}$$

where

$$U_{11} = -\frac{\psi_2\dot{\theta}_0 - \dot{\phi}_0}{(\psi_1-\psi_2)\omega_1} \tag{28}$$

$$U_{12} = -\frac{(\theta_0\psi_2 - \phi_0)(C+D-g) + a_{\max}(\psi_2-1)}{(C+D-g)(\psi_1-\psi_2)} \tag{29}$$

$$U_{21} = \frac{\psi_1\dot{\theta}_0 - \dot{\phi}_0}{n\omega_1(\psi_1-\psi_2)} \tag{30}$$

$$U_{22} = \frac{(\theta_0\psi_1 - \phi_0)(C+D-g) + a_{\max}(\psi_1-1)}{(C+D-g)(\psi_1-\psi_2)}, \tag{31}$$

where θ_0 is the initial angle and $\dot{\theta}_0$ is the initial angular velocity for the angle θ, while ϕ_0 is the initial angle and $\dot{\phi}_0$ is the initial angular velocity for the angle ϕ. Equations (26)–(31) represent the general solutions for the linear equations of motion of a double pendulum (3), which can be utilized to produce the acceleration profile specified in Equation (9). It is evident that θ and ϕ retain three distinct formulas during the acceleration stage. These formulas depend on the initial angles and initial angular velocities, as illustrated in Equations (28)–(31). The applied acceleration has a constant value of $a_{\max}$ during the first phase, zero in the second phase, and returns to $a_{\max}$ in the third phase. At the beginning of each stage, four initial conditions are required as inputs: θ_0, $\dot{\theta}_0$, ϕ_0, and $\dot{\phi}_0$. During the initial phase, both initial angles and initial angular velocities are set to zero as the motion begins from a state of rest. Using the equations formed in the first stage, the initial angles and angular velocities for the second stage are found at the end of the first stage. Similarly, in the third stage, the initial angles and angular velocities are found at the end of the second stage.

4 | Numerical and Experimental Validation

To increase the efficiency of rest-to-rest maneuvers, many industrial operations depend on the uncontrolled, TORB as the most straightforward and fastest maneuver. In this maneuver, the acceleration time is defined as $t_a = a_{\max}/v_{\max}$ where $a_{\max}$ is the maximum chosen acceleration for the controller and $v_{\max}$ is the required maximum velocity of the trolley; see Figure 2. However, using such a maneuver results in significant residual vibrations at the end of the maneuver.

To eliminate residual vibrations induced in a single-mode system, the acceleration time, t_a, is divided equally into two phases with the same amplitude, as shown in Figure 2. The second stage is delayed by half the oscillation period of the payload, T, to counteract the induced vibration generated by the acceleration of the first stage. The time to start the second acceleration stage can be mathematically written as $T/2 = \pi/\omega$. This technique is usually used for single-mode systems and is called the single-mode double-step input shaper (SMDS).

To illustrate the effectiveness of the proposed technique and the shortcomings of the double-step shaper to control a double pendulum, two scenarios with randomly chosen lengths and masses are simulated numerically and tested experimentally on a scaled overhead crane in the Advanced Vibration Lab at Kuwait University, as shown in Figure 3.

The experimental crane has a DC motor to move the crane's trolley. Three quadrature incremental encoders are used to assess trolley movement, the length of the hoist cable, and the oscillation angle of the hoisting cable. Each encoder has a resolution of 1024 pulses per revolution. An interface between a PC and the crane system is established using an RT-DAC/PCI multipurpose digital I/O board. The interface software utilizes MATLAB's real-time Simulink environment. The control hardware has a sampling rate of 100 Hz. The maximum trolley velocity and acceleration are tested as 0.35 m/s and 1.5 m/s^2, respectively. The crane has a usable track of 0.6 m.

The parameters of the system for both examples are shown in Table 1. In the first example, the masses, m_1 and m_2, are selected as 0.055 kg and 0.11 kg, respectively. The cable lengths are selected as $l_1 = 0.30$ m and $l_2 = 0.10$ m. The maximum velocity is set at 0.30 m/s, while the final distance is set to 0.45 m. For the second example, the maximum velocity and final distance remain the same while the masses are randomly chosen as $m_1 = 0.055$ kg and $m_2 = 0.21$ kg. The cable lengths are selected as $l_1 = 0.30$ m and $l_2 = 0.20$ m.

To understand the need for an input shaper to reduce residual vibrations, an uncontrolled (TORB) shaper is used to move the trolley to the desired location using the assigned maximum velocity. The profiles for the first and the second examples are shown in Figure 4. For both cases, it is clear that the final velocity is reached accurately at the end of the acceleration phase, and the final position is achieved at the end of motion. The response of the first angle, θ, is calculated numerically and measured experimentally. Examining Figure 5A,B, it is clear that both the experimental and the simulated results showed very large residual vibrations at the end of the maneuver. It is

TABLE 1 | Numerical values of the system's parameters simulated in the two cases.

	Case 1	Case 2
m_1 [kg]	0.055	0.055
m_2 [kg]	0.11	0.21
l_1 [m]	0.30	0.30
l_2 [m]	0.10	0.20
ω_1 [rad/s]	5.127	4.551
ω_2 [rad/s]	19.134	19.318
ω_2/ω_1	3.732	4.245
$v_{\max}$ [m/s]	0.30	0.30

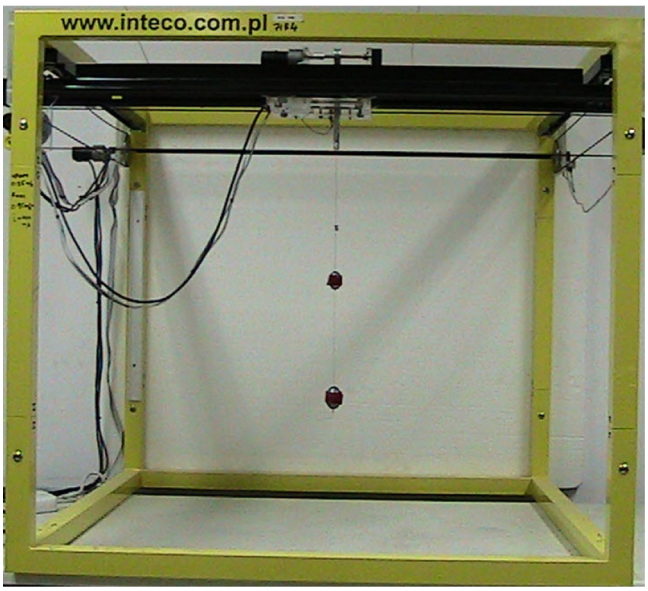

FIGURE 3 | INTCO experimental setup at Kuwait University Advanced Vibration Lab.

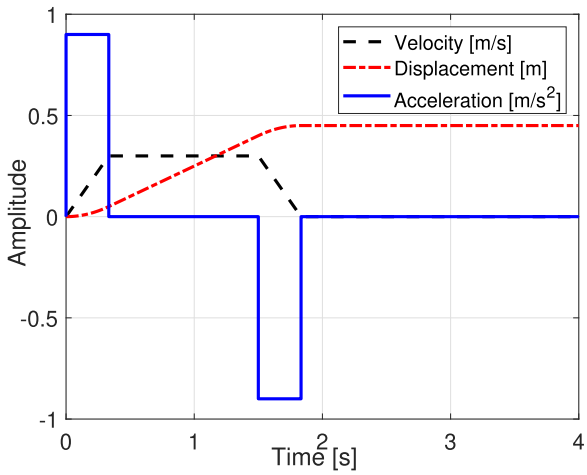

FIGURE 4 | Time optimal rigid body (TORB) acceleration, velocity, and displacement profiles.

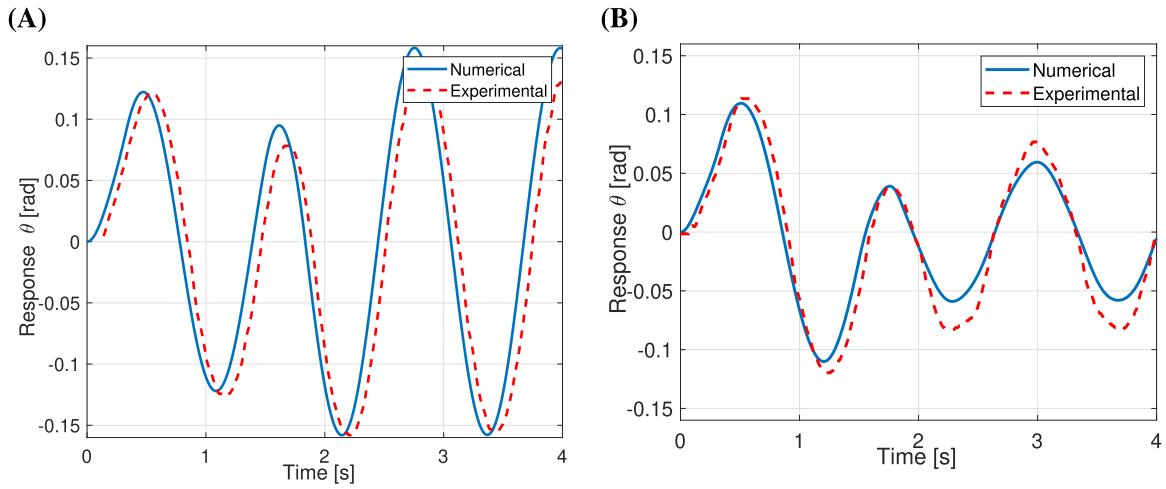

FIGURE 5 | Time-optimal rigid body (TORB) numerical and experimental profiles and responses for case 2.

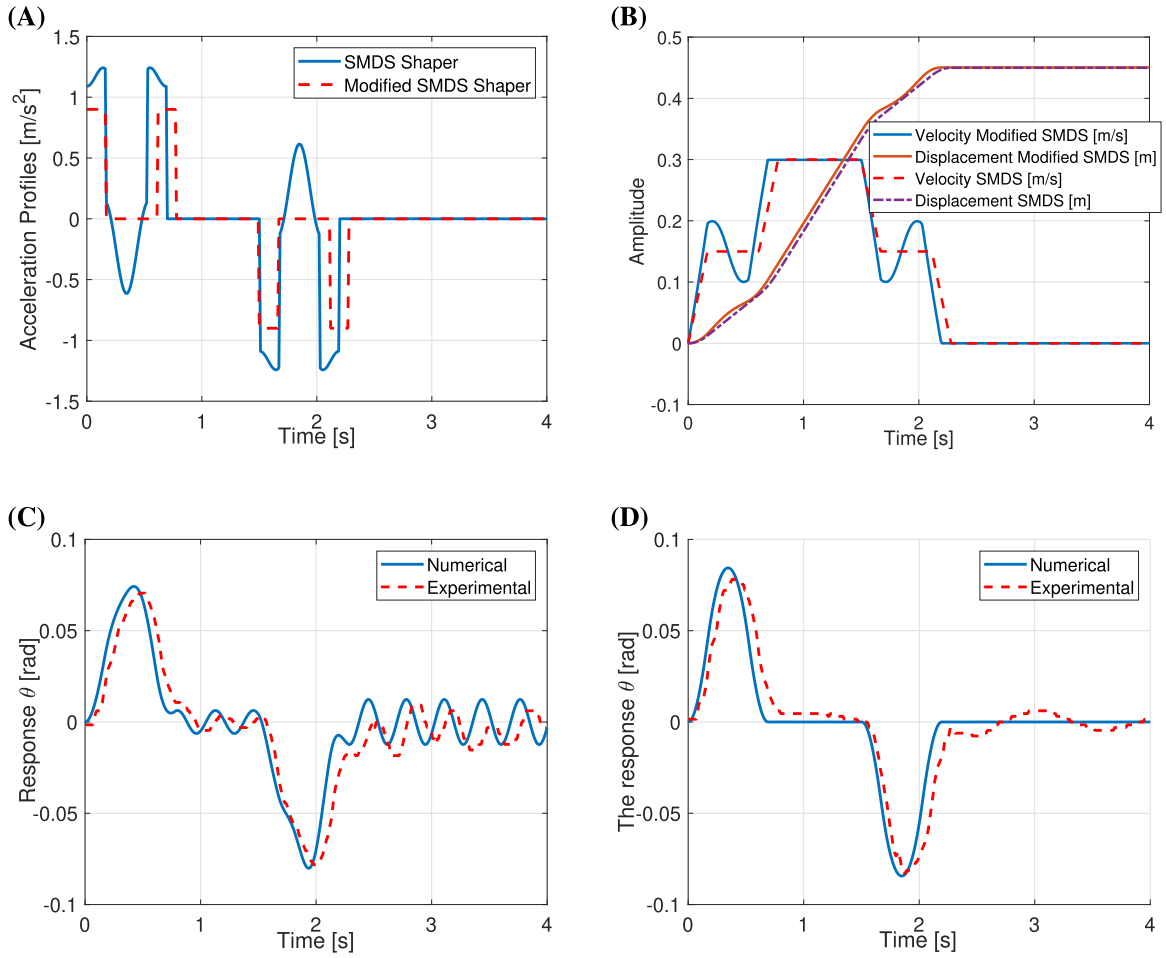

FIGURE 6 | (A) Controlled and uncontrolled acceleration profiles. (B) Controlled and uncontrolled velocity and displacement profiles. (C) Numerical and experimental responses for uncontrolled Case 1. (D) Numerical and experimental responses for controlled Case 1.

also clear that the experimental and numerical results are in good agreement for both cases.

To reduce these vibrations, a SMDS input shaper is utilized and then modified to eliminate all the residual induced vibrations. It is well known that applying a single-mode input shaper to a double pendulum results in considerable unwanted residual oscillations, particularly in the second mode. The acceleration profile of a SMDS input shaper, featuring a maximum acceleration of 0.9 m/s^2, is applied to the trolley, as illustrated in Figure 6A. The velocity and displacement profiles of the single-mode input shaper are shown in Figure 6B. It is clear that the cruising velocity is achieved accurately and the final distance is reached. Examining the responses plotted in Figure 6C, the performance of the single mode shaper considerably reduced the residual vibrations compared to the (TORB) response, Figure 5A.

However, the experimental and numerical residual vibrations of the second mode are clearly observed.

To eliminate the residual vibrations of both modes, the proposed technique is implemented. As shown in Table 1, the unmodified system frequency ratio is 3.732. Utilizing Equations (18) and (19), the value of the first natural frequency is chosen as 6.00 rad/s, and the ratio n is chosen as 3. The gains C and D are then calculated using Equations (20) and (21) as 9.72 and −11.799, respectively. Using the calculated parameters to generate the shaper profiles, the new acceleration profile is generated using Equations (9), (26), and (27). The modified acceleration profiles are compared to the original (SMDS) profile in Figure 6A. Small changes to the original (SMDS) acceleration profile are noticed. It is clear that the modified profile increases the maximum acceleration by almost 30%. To ensure accurate maneuver, the velocity and position profiles of the trolley are plotted and compared with the (SMDS) profiles in Figure 6B. The trolley's velocity and displacement profiles have small changes compared to the (SMDS) profiles, which will have very small effects on the crane's actuators. The target position of $u = 0.450$ m is achieved with exceptional accuracy. The system's response under the proposed shaper is shown in Figure 6D. It is evident that the proposed shaper completely eliminated residual vibrations. As expected, very small differences are noticed between the numerical and experimental results due to many factors such as delay, friction, motor backlash, and so forth.

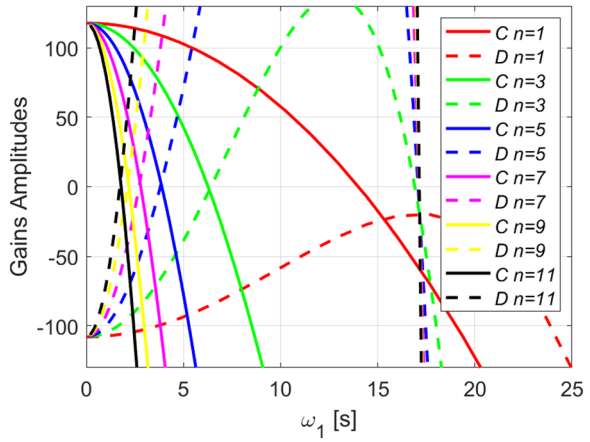

FIGURE 7 | The gain values of C and D for Case 1.

In the previous example, the value of the modified natural frequency is chosen randomly. This random selection may result in the values of the controller gains C and D being

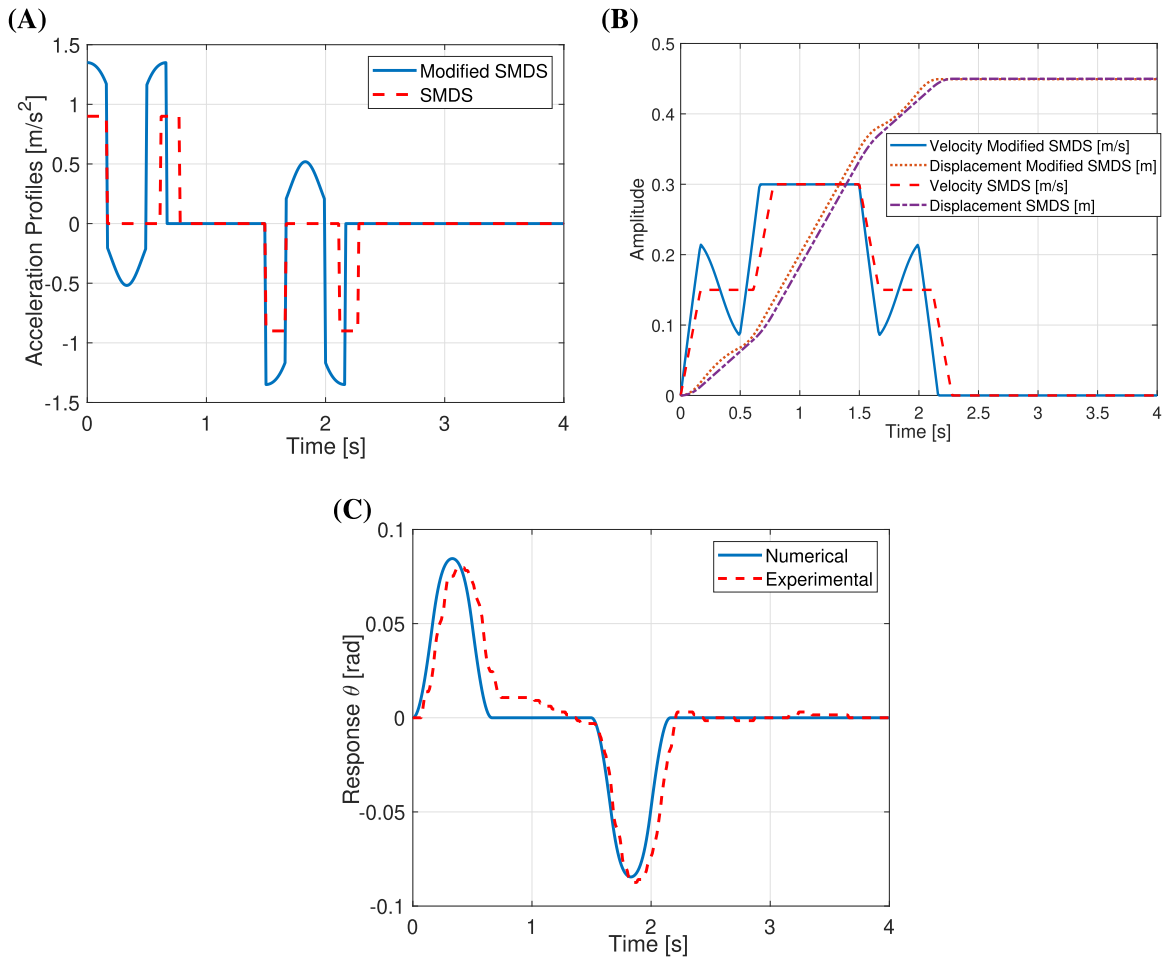

FIGURE 8 | (A) Controlled and uncontrolled acceleration profiles. (B) Controlled and uncontrolled velocity and displacement profiles. (C) Numerical and experimental responses for controlled Case 1.

relatively large. These large values may increase the acceleration requirements needed to move the trolley; see Equation (9). To better choose the value of the modified first natural frequency $\bar{\omega}_1$, Equations (20) and (21) are plotted as functions of the first natural frequency modified in Figure 7 with different values of n. It is observed that D starts at a large negative value and then increases with the increase of $\bar{\omega}_1$. However, the value of C starts from a large positive value and decreases as the value of $\bar{\omega}_1$ increases. To have the minimum value for both gains, the value of $\bar{\omega}_1$ is chosen at the intersection between the two curves. For Case 1, the intersection values and the modified frequency are shown in Table 3 using different values of n. For $n = 3$, the intersection value gives $\bar{\omega}_1 = 6.329$ rad/s, while the value of the gains C and D is -2.456, as illustrated in Table 3.

To test the new gain values on the system performance, the acceleration profiles for both the proposed shaper and the classical (SMDS) are plotted in Figure 8A. It is clear that the modified acceleration profile is slightly changed. As shown in Figure 8B, the velocity and displacement profiles are compared with the classical (SMDS) profiles. Clearly, the proposed shaper managed to reach the maximum velocity and final

TABLE 2 | Numerical values of the controller's parameters simulated in the two cases.

	Case 1 Un	Case 1a	Case 1b	Case 2	Case 2a	Case 2b
$a_{\max}\left[\mathrm{m/s^2}\right]$	0.9	1.089	0.055	0.9	0.7425	0.6480
t_c[s]	0.72	0.8136	1.1667	0.6350	0.5397	0.5150
ω_1[rad/s]	5.127	6.00	6.3292	4.551	4.00	3.8700
ω_2[rad/s]	19.134	18.00	18.9876	19.318	20.00	19.3500
$\frac{\omega_1}{\omega_2}$	3.732	3.00	3.00	4.245	5.00	5.00
The gain C	0.00	9.7200	−2.4560	0.00	−6.6341	1.3458
The gain D	0.00	−11.7999	−2.4560	0.00	8.3199	1.3458

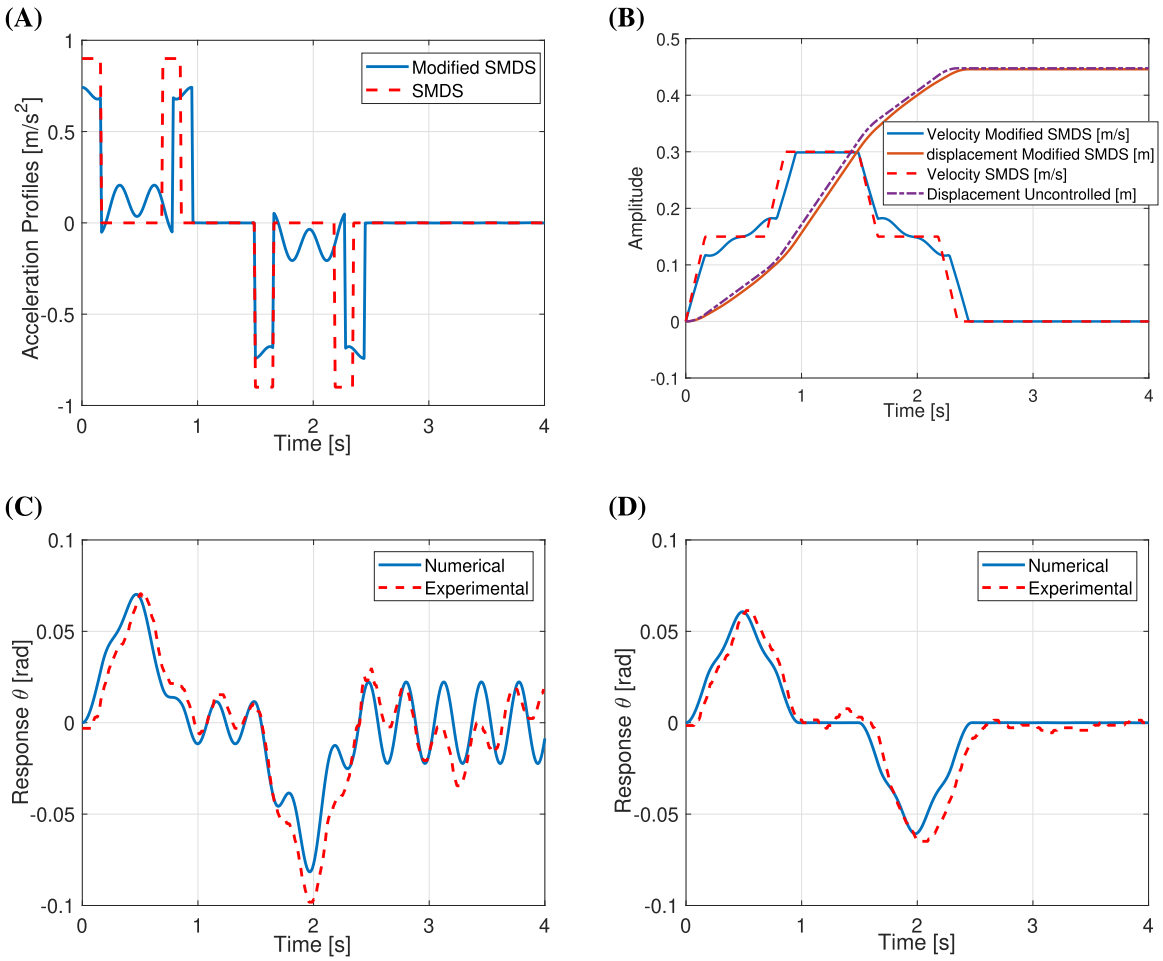

FIGURE 9 | (A) Controlled and uncontrolled acceleration profiles. (B) Controlled and uncontrolled velocity and displacement profiles. (C) Numerical and experimental responses for uncontrolled Case 2. (D) Numerical and experimental responses for controlled Case 2.

position with precision. As shown in Figure 6C, applying the classical shaper (SMDS) resulted in undesired residual vibrations at the end of the maneuver. Testing the response of the system with the modified shaper eliminates the residual vibration of the system, as shown in Figure 8C.

The second example follows an identical approach to determine the controller gains C and D, as shown in Table 2. The first natural frequency is chosen as $\bar{\omega}_1 = 4.00\,\text{rad/s}$ and since the frequency ratio of the original system is 4.245, the value of n is selected as 5.0. The new natural frequencies of the system are $\omega_1 = 4$ and $\omega_2 = 20.00$. The acceleration profile of the modified shaper is plotted and compared to the (SMDS) acceleration profile in Figure 9A. In this case, the value of the controller's maximum acceleration is smaller than the maximum acceleration used by the (SMDS) shaper. In Figure 9B, small changes are observed in the velocity and displacement profiles. However, the cruising velocity and the final displacement are accurately reached. As shown in the previous example, the (SMDS) shaper manages to reduce residual vibrations but fails to eliminate them, as shown in Figure 9C. The numerical and experimental results show that the newly proposed shaper successfully eliminated the residual vibration, as evident in Figure 9D.

To optimize the values of the gains C and D, Equations (20) and (21) for Case 2 are plotted as a function of $\bar{\omega}_1$ in Figure 10. The same behavior is observed for C and D, as in the first case. The two curves for $n = 5$ intersect at $\bar{\omega}_1 = 3.8700\,\text{rad/s}$, leading to an equal value of the gains where $C = D = 1.3458$, as listed in Table 3. To test the shaper with the new gains, the acceleration of the resulting shaper is compared to the classical shaper (SMDS) in Figure 11A. Small alterations are noticed between the two profiles. The controller's maximum acceleration is reduced since the gain values are positive. The velocity and displacement profiles are plotted in Figure 11B. As discussed previously, the experimental and numerical results, plotted in Figure 9C, clearly indicate that the classical (SMDS) shaper does not eliminate residual vibration. To test the modified shaper, the numerical and experimental results of the proposed shaper are plotted in 11C. It is clear that the proposed shaper completely eliminates the residual vibrations at the end of the motion.

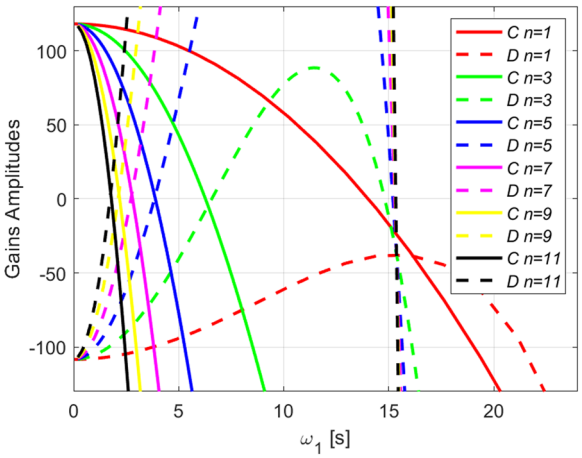

FIGURE 10 | The gain values of C and D for Case 2.

The presented results demonstrate the efficacy of the proposed technique through four examples tested numerically and experimentally. In the presented examples, the residual vibration amplitude of the (SMDS) shaper has been significantly reduced, going from around 0.06 rad to close to zero.

5 | Conclusions

A SMDS input shaper can eliminate residual vibrations in multi-mode systems, provided that the higher frequency is an odd multiple of the fundamental frequency. This study modified a (SMDS) input shaper to eliminate residual vibrations in a two-degree-of-freedom system. The modification involves incorporating scaled responses of the first angle θ and the second angle ϕ into the original shaper to adjust the natural frequencies of the system. Since the proposed shaper added two scaled constants, two constraints can be utilized. The first constraint allows the user to select the fundamental frequency while the second constraint is used to force the higher frequency to be an odd multiple of the fundamental frequency. The equations of motion for a double pendulum are found, linearized, and solved analytically. Upon satisfying the constraints mentioned above, the scaling factors C and D are analytically determined.

To prove the concept, two experimentally and numerically simulated scenarios with arbitrary parameters are presented. The experimental and simulation results indicate that using the unmodified (SMDS) shaper fails to eliminate all the induced vibrations, especially, residual vibration induced by higher

TABLE 3 | Numerical values of the controller's frequencies as a function of n.

n	D and C Case 1	ω_1 Case 1	ω_2 Case 1	D and C Case 2	ω_1 Case 2	ω_2 Case 2
1	−23.2173	15.3263	15.3263	−38.2051	16.1437	16.1437
3	−2.4560	6.3292	18.9876	−4.6721	6.3989	19.1967
5	2.1055	3.8500	19.2499	1.3458	3.8700	19.3500
7	3.4558	2.7600	19.3200	3.0741	2.7700	19.3899
9	4.0231	2.1498	19.3486	3.7937	2.1562	19.4060
11	4.3129	1.7603	19.3630	4.1598	1.7649	19.4140
13	4.4803	1.4901	19.3712	4.3710	1.4937	19.4140

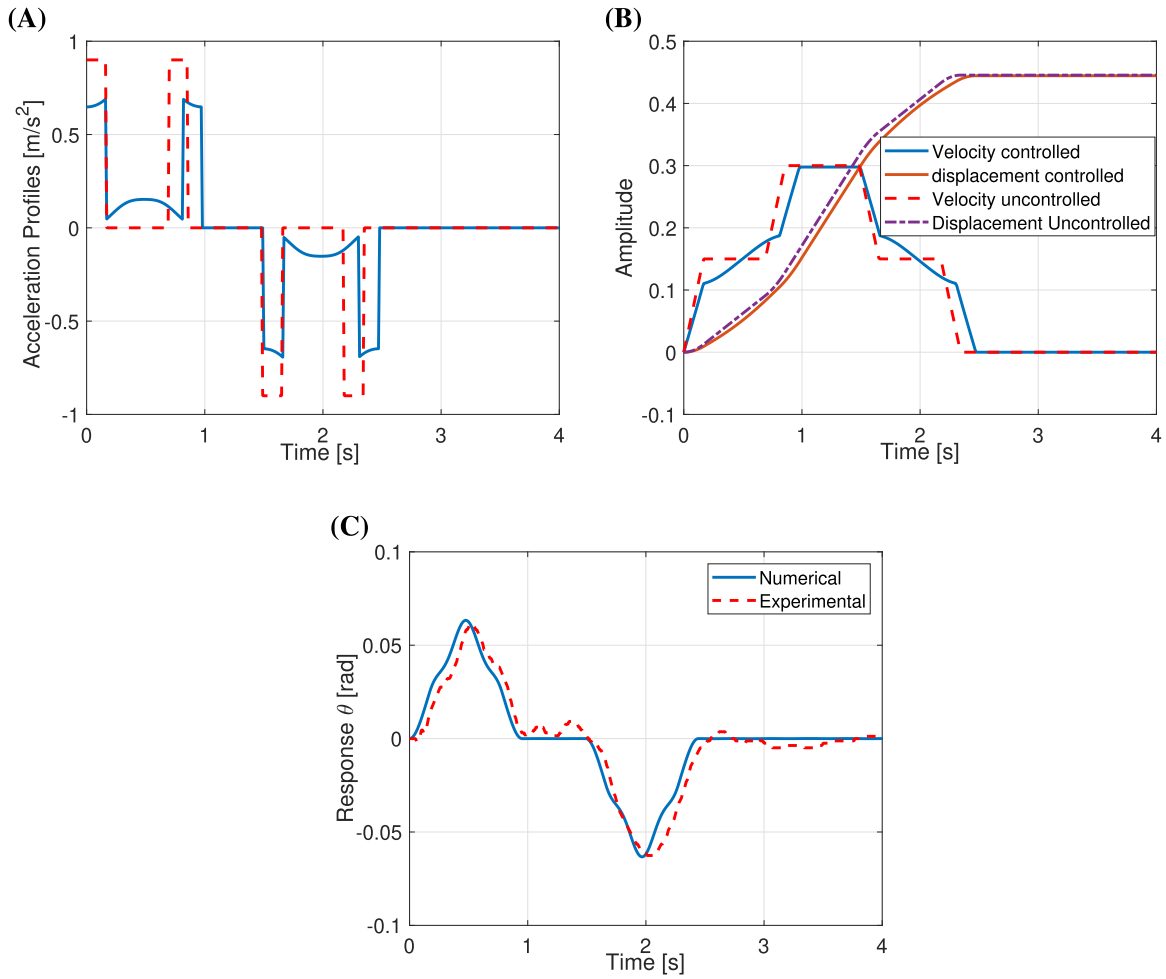

FIGURE 11 | (A) Controlled and uncontrolled acceleration profiles. (B) Controlled and uncontrolled velocity and displacement profiles. (C) Numerical and experimental responses for controlled Case 2.

modes. On the other hand, the proposed technique successfully eliminates the residual vibrations in both modes of a double pendulum. It is worth noting that, the primary benefit of analytical derivation is the elimination of complex numerical or optimization methods. Furthermore, and with more complicated calculations, this technique can be implemented on any multimode system.

Acknowledgments

This study is funded by Kuwait University Research Sector EM04/24.

Conflicts of Interest

The author declares no conflicts of interest.

Data Availability Statement

The data that support the findings of this study are available on request from the corresponding author. The data are not publicly available due to privacy or ethical restrictions.

References

1. E. M. Abdel-Rahman, A. H. Nayfeh, and Z. N. Masoud, "Dynamics and Control of Cranes: A Review," *Journal of Vibration and Control* 9, no. 7 (2003): 863–908.

2. W. Singhose, "Command Shaping for Flexible Systems: A Review of the First 50 Years," *International Journal of Precision Engineering and Manufacturing* 10, no. 4 (2009): 153–168.

3. J. Vaughan, A. Yano, and W. Singhose, "Comparison of Robust Input Shapers," *Journal of Sound and Vibration* 315, no. 4 (2008): 797–815.

4. K. L. Sorensen, W. Singhose, and S. Dickerson, "A Controller Enabling Precise Positioning and Sway Reduction in Bridge and Gantry Cranes," *Control Engineering Practice* 15, no. 7 (2007): 825–837.

5. Z. N. Masoud, K. A. Alhazza, M. A. Majeed, and E. A. Abu-Nada, eds., "A Hybrid Command-Shaping Control System for Highly Accelerated Double-Pendulum Gantry Cranes," in *7th International Conference on Multibody Systems, Nonlinear Dynamics, and Control, Parts A, B and C, Volume 4 of International Design Engineering Technical Conferences and Computers and Information in Engineering Conference* (ASME, 2009), 1809–1817.

6. N. Nagal, S. Srivastava, C. Pandey, A. Gupta, and A. K. Sharma, "Alleviation of Residual Vibrations in Hard-Magnetic Soft Actuators Using a Command-Shaping Scheme," *Polymers* 14, no. 15 (2022): 16575.

7. K. Golwala, R. A. Boby, and A. Kumar Sharma, eds., " Alleviation of Viscoelastic Creep in Electrostatically Driven Soft Dielectric Elastomer Actuators Using Input Shaping Scheme," in *2024 20th IEEE/ASME International Conference on Mechatronic and Embedded Systems and Applications* (MESA, 2024), 1–8.

8. A. K. Sharma, "Design of a Command-Shaping Scheme for Mitigating Residual Vibrations in Dielectric Elastomer Actuators," *Journal of Applied Mechanics* 87, no. 2 (2019): 021007.

9. R. K. Godara and M. M. Joglekar, "Mitigation of Residual Oscillations in Electrostatically Actuated Microbeams Using a Command-Shaping Approach," *Journal of Micromechanics and Microengineering* 25, no. 11 (2015): 115028.

10. W. Singhose and L. Pao, "A Comparison of Input Shaping and Time-Optimal Flexible-Body Control," *Control Engineering Practice* 5, no. 4 (1997): 459–467.

11. W. E. Singhose, R. Eloundou, and J. Lawrence, "Command Generation for Flexible Systems by Input Shaping and Command Smoothing," *Journal of Guidance Control and Dynamics* 33, no. 6 (2010): 1697–1707.

12. Y. G. Sung and S. Lee, "Robust Input Shaping Commands With First-Order Actuators," *Micromachines* 15, no. 9 (2024): 15091086.

13. K. A. Alhazza and Z. N. Masoud, eds., "A Novel Wave-Form Command-Shaping Control With Application on Overhead Cranes," in *Dynamic Systems and Control Conference*, 44182 (2010), 331–336.

14. Z. N. Masoud and K. A. Alhazza, "A Smooth Multimode Waveform Command Shaping Control With Selectable Command Length," *Journal of Sound and Vibration* 397, no. 4 (2017): 1–16.

15. K. Alhazza and Z. Masoud, "A Novel Wave-Form Command-Shaper for Overhead Cranes," *Journal of Engineering Research* 1, no. 3 (2013): 181–209.

16. K. A. Alhazza, A. H. Al-Shehaima, and Z. N. Masoud, eds., " A Continuous Modulated Wave-Form Command Shaping for Damped Overhead Cranes," in *8th International Conference on Multibody Systems, Nonlinear Dynamics, and Control, Parts A and B, Volume 4 of International Design Engineering Technical Conferences and Computers and Information in Engineering Conference* (ASME, 2011), 361–366.

17. K. A. Alhazza, "Adjustable Maneuvering Time Wave-Form Command Shaping Control With Variable Hoisting Speeds," *Journal of Vibration and Control* 23, no. 7 (2017): 1095–1105.

18. M. Alfares, K. Alhazza, and A. Alawadhi, "A Waveform Command Shaping Control of a Damped Single Degree-of-Freedom Crane System With Nonzero Initial Conditions," *International Journal of Dynamics and Control* 28, no. 8 (2024): 2850–2863.

19. K. A. Alhazza, M. Alfares, and A. Alawadhi, eds., "A Closed-Form Command Shaping Control of a Rotating Flexible Beam With Nonzero Initial Conditions," in *19th International Conference on Multibody Systems, Nonlinear Dynamics, and Control (MSNDC), Volume 10 ofInternational Design Engineering Technical Conferences and Computers and Information in Engineering Conference* (ASME, 2023), V010T10A025.

20. K. A. Alhazza, Z. N. Masoud, and J. A. Alqabandi, "A Close-Form Command Shaping Control for Point-to-Point Maneuver With Nonzero Initial and Final Conditions," *Mechanical Systems and Signal Processing* 170, no. 7 (2022): 108804.

21. M. Alfares and K. Alhazza, "Comparative Analysis on the Performance of Different Types of Input- and Command-Shaping Controllers in Minimizing Payload Residual Vibration of an Overhead Crane With an Inclined Supporting Track," *International Journal of Mechanical System Dynamics* 4, no. 1 (2024): 22–33.

22. D. Newman, S. W. Hong, and J. E. Vaughan, "The Design of Input Shapers Which Eliminate Nonzero Initial Conditions," *Journal of Dynamic Systems, Measurement, and Control* 140, no. 10 (2018): 101005.

23. T. S. Amer, R. Starosta, A. S. Elameer, and M. A. Bek, "Analyzing the Stability for the Motion of an Unstretched Double Pendulum Near Resonance," *Applied Sciences* 11, no. 20 (2021): 9520.

24. F. El-Sabaa, T. Amer, H. Gad, and M. Bek, "Novel Asymptotic Solutions for the Planar Dynamical Motion of a Double-Rigid-Body Pendulum System Near Resonance," *Journal of Vibration Engineering & Technologies* 10, no. 5 (2022): 1955–1987.

25. M. Alfares and K. Alhazza, "A Waveform Command Shaping Control of a Double Pendulum With Nonzero Initial Conditions," *Asian Journal of Control* 26, no. 4 (2024): 1849–1863.

26. T. Amer, G. M. Moatimid, S. Zakria, and A. Galal, "Vibrational and Stability Analysis of Planar Double Pendulum Dynamics Near Resonance," *Nonlinear Dynamics* 112, no. 24 (2024): 21667–21699.

27. A. Amer, W. Zhang, T. Amer, and H. Li, "Nonlinear Vibration Analysis of a 3DOF Double Pendulum System Near Resonance," *Alexandria Engineering Journal* 113, no. 2 (2025): 262–286.

28. M. H. Shaheed, M. O. Tokhi, A. J. Chipperfield, and A. K. M. Azad, "Modelling and Open-Loop Control of a Single-Link Flexible Manipulator With Genetic Algorithms," *Journal of Low Frequency Noise, Vibration and Active Control* 20, no. 1 (2001): 39–55.

29. S. Rhim and W. Book, "Adaptive Time-Delay Command Shaping Filter for Flexible Manipulator Control," *IEEE/ASME Transactions on Mechatronics* 9, no. 4 (2004): 619–626.

30. Z. Mohamed and M. Tokhi, "Command Shaping Techniques for Vibration Control of a Flexible Robot Manipulator," *Mechatronics* 14, no. 1 (2004): 69–90.

31. J. Hyde and W. Seering, "Using Input Command Pre-Shaping to Suppress Multiple Mode Vibration," *Proceedings 1991 IEEE International Conference on Robotics and Automation* 3 (1991): 2604–2609.

32. J. M. Hyde and W. P. Seering, eds., " Inhibiting Multiple Mode Vibration in Controlled Flexible Systems," in *1991 American Control Conference* (1991), 2449–2454.

33. J. Vaughan, D. Kim, and W. Singhose, "Control of Tower Cranes With Double-Pendulum Payload Dynamics," *IEEE Transactions on Control Systems Technology* 18, no. 6 (2010): 1345–1358.

34. A. Alshaya and K. Alhazza, "Smooth and Robust Multi-Mode Shaped Commands," *Mechanical Systems and Signal Processing* 168, no. 1 (2022): 108658.

35. Z. N. Masoud and K. A. Alhazza, eds., "Command-Shaping Control System for Double-Pendulum Gantry Cranes," in *8th International Conference on Multibody Systems, Nonlinear Dynamics, and Control, Parts A and B* (International Design Engineering Technical Conferences and Computers and Information in Engineering Conference, 2011), 367–375.

36. Z. N. Masoud and K. A. Alhazza, "Frequency-Modulation Input Shaping Control of Double-Pendulum Overhead Cranes," *Journal of Dynamic Systems Measurement and Control-transactions of the Asme* 136, no. 2 (2014): 021005.

37. Z. Masoud, K. Alhazza, E. Abu-Nada, and M. Majeed, "A Hybrid Command-Shaper for Double-Pendulum Overhead Cranes," *Journal of Vibration and Control* 20, no. 1 (2014): 24–37.

38. S. Arabasi and Z. Masoud, "Frequency-Modulation Input-Shaping Strategy for Double-Pendulum Overhead Cranes Undergoing Simultaneous Hoist and Travel Maneuvers," *IEEE Access* 10, no. 3 (2022): 44954–44963.

39. S. Arabasi and Z. N. Masoud, "Simultaneous Travel and Hoist Maneuver Input Shaping Control Using Frequency Modulation," *Shock and Vibration* 2017 (2017): 1–12.

40. K. A. Alhazza, ed., "A New Frequency-Modulation Input-Shaping Strategy Applied on a Double-Pendulum," in *20th International Conference on Multibody Systems, Nonlinear Dynamics, and Control (MSNDC)* (International Design Engineering Technical Conferences and Computers and Information in Engineering Conference, 2024).